以調變 Wavelet 轉換進行紋理影像的分割
Texture Segmentation by Modulated Wavelet Transform

辛 錫 進
Hsi-Chin Hsin

Department of Electrical Engineering
Chung-Hua University
hsin@chu.edu.tw

摘要

本文以調變的方式發展出一個具有方向辨別性的轉換技術，稱之爲調變 wavelet 轉換，以紋理影像的分割爲例，展現其應用的潛力。

關鍵字：Wavelet 轉換，紋理分割

Abstract

The modulated wavelet transform has been developed which provides the orientation selectivity to improve the segmentation performance of textured images. The potential is shown by experimental results.

Keywords: Wavelet transform, texture segmentation

1. Introduction

The local changes of signals can be characterized by the short time Fourier transform where the joint time/frequency resolution depends on the window utilized. Gaussian window has the optimum joint resolution property such that a set of Gabor filters has been developed for texture analysis and segmentation [1]-[3]. However, the tuning of the parameters requires a prior analysis and experimental decision. Unser and Eden use a series of Gaussian smooth windows with a half octave scale progression to estimate features in multiple resolutions for segmenting textures [4]. Bouman and Liu propose a resolution progressive scheme by segmenting the textured image starting at the coarsest resolution to guide the successive segmentation until the finest resolution is reached [5]. Krishnamachari and Chellappa develop a multiresolution Gauss Markov random field (GMRF) modeling for texture segmentation [6] for reducing the computational load caused by single resolution MRF modeling [7],[8]. Recently, wavelet theory has been developed enabling an efficient decomposition of signals to provide both time/space and frequency localization [9]-[11]. The (standard) wavelet transform focuses on the successive decomposition in the low frequency region, however, the dominant spatial frequencies of textures are usually in the middle frequency region. A tree structured wavelet transform has been developed to extend the decomposition into the high frequency region [12]. This approach appears to be similar to the wavelet packet method which has been applied to texture classification [13]. Both approaches are limited in the orientation selectivity since the textures of $+6$ and -6 orientations can not be discriminated. Hsin and Li develop a segmentation method featuring orientation selectivity, in a multiresolution manner, based on a set of numerically acceptable 2D wavelets constructed by modulating a valid 2D scaling function in different orientations [14]. In this paper, the exact decomposition and reconstruction of signals and images using modulated wavelets is developed and applied to detecting the emergent frequency of signals and segmenting textured images.

2. 1D Wavelet Transform

There is a wavelet, $\psi(x)$, whose scaled and translated versions form a basis for the set of finite energy signals, $L^2(R)$. The detail space W_j defined by $\{\psi_{jn}(x)\}_{n\in Z}$, where $\psi_{jn}(x) = 2^{-j/2}\psi(2^{-j}x-n)$ is the scaled version of $\psi(x)$ at resolution 2^j translated to position n, partitions $L^2(R)$ in the sense of $L^2(R) = \overline{\oplus_{j=-\infty}^{\infty} W_j}$, where $\oplus$ is the direct sum and over-line is the closure operator. The subset V_j defined by $\oplus_{i=j+1}^{\infty} W_i$ is called the approximation space of $L^2(R)$ at resolution 2^j. One can find a scaling function $\phi(x)$ such that $\{\phi_{jn}(x)\}_{n\in Z}$ forms a basis for V_j ($\phi_{jn}(x) = 2^{-j/2}\phi(2^{-j}x-n)$). The sequence of $\{V_j\}_{j\in Z}$ provides a multiresolution analysis (MRA) of $L^2(R)$ in the sense

of $V_{J+1} \subseteq V_j$ (net structure), and $\overline{\bigcup_{\ell} V_\ell} = L^2(R)$ [9]. It is noted that, in our definition, a large scale index ℓ means a coarse resolution. For a signal $f(x) \in V_0$ decomposed by

$$f(x) = \sum_n S_J(n)\phi_{Jn}(x) + \sum_{\ell=J}^{1}\sum_n D_\ell(n)\psi_{\ell n}(x) \qquad (1)$$

where $S_\ell(n)$ and $D_\ell(n)$ are the scaling coefficient and wavelet coefficient at resolution 2^ℓ, position n, respectively and J is the coarsest scale in decomposition. The scaling coefficients and wavelet coefficients at coarse resolution can be computed by applying the standard wavelet transform on the scaling coefficients at the next finer resolution as follows,

$$\begin{aligned} S_\ell(n) &= \sum_k S_{\ell-1}(k)h(2n-k) \\ D_\ell(n) &= \sum_k S_{\ell-1}(k)g(2n-k) \end{aligned} \qquad (2)$$

where $h(-n) = \tilde{h}(n) = <\phi(x), \phi_{-1n}(x)>$ and $g(-n) = \tilde{g}(n) = <\psi(x), \phi_{-1n}(x)>$. The standard inverse wavelet transform is then given by

$$S_{\ell-1}(n) = \sum_k S_\ell(k)\tilde{h}(n-2k) + \sum_k D_\ell(k)\tilde{g}(n-2k) \qquad (3)$$

which means that the scaling coefficients at fine resolution can be exactly reconstructed from the scaling coefficients and wavelet coefficients at the next coarser resolution.

3.1 1D Modulated Wavelet Transform

Let us consider a signal of the form $f(x)e^{jUx}$ where $f(x) \in V_0$ is a smooth signal modulated by U and the subspace V_0 corresponds to a valid scaling function $\phi(x)$. By the decomposition of $f(x)$ (equation (1)), it is shown that

$$\begin{aligned} f(x)e^{jUx} = &\sum_n (S_J(n)e^{j2^J Un})\phi_{Jn}(x)e^{j2^J U(2^{-J}x-n)} \\ &+ \sum_{\ell=J}^{1}\sum_n (D_\ell(n)e^{j2^\ell Un})\psi_{\ell n}(x)e^{j2^\ell U(2^{-\ell}x-n)} \end{aligned} \qquad (4)$$

where $\phi_{\ell n}(x)\ e^{j2^\ell U(2^{-\ell}x-n)}$ and $\psi_{\ell n}(x)\ e^{j2^\ell U(2^{-\ell}x-n)}$ can be considered to be the modulated scaling function and the modulated wavelet by frequency $2^\ell U$ at resolution 2^ℓ, respectively $(S_\ell(n)e^{j2^\ell Un})$ and $(D_\ell(n)\ e^{j2^\ell Un})$ are the associated scaling coefficients and wavelet coefficients with respective to the decomposition of the signal $f(x)e^{jUx}$. Based on the standard wavelet transform of $f(x)$ (equation (2)), $(S_\ell(n)e^{j2^\ell Un})$ and $(D_\ell(n)e^{j2^\ell Un})$ can be computed directly from the coefficients $(S_{\ell-1}(n)e^{j2^{\ell-1}Un})$ as follows,

$$\begin{aligned} &S_\ell(n)e^{j2^\ell Un} = \\ &\quad \sum_k (S_{\ell-1}(k)e^{j2^{\ell-1}Uk})(h(2n-k)e^{j2^{\ell-1}U(2n-k)}) \\ &D_\ell(n)e^{j2^\ell Un} = \\ &\quad \sum_k (S_{\ell-1}(k)e^{j2^{\ell-1}Uk})(g(2n-k)e^{j2^{\ell-1}U(2n-k)}) \end{aligned} \qquad (5)$$

which is called the modulated wavelet transform. Similarly, based on equation (3), the modulated inverse wavelet transform is given by

$$\begin{aligned} S_{\ell-1}(n)e^{j2^{\ell-1}Un} = &\sum_k S_\ell(k)e^{j2^\ell Uk}\tilde{h}(n-2k)e^{j2^{\ell-1}U(n-2k)} + \\ &\sum_k D_\ell(k)e^{j2^\ell Uk}\tilde{g}(n-2k)e^{j2^{\ell-1}U(n-2k)} \end{aligned} \qquad (6)$$

3.2 Emergent Frequency Detection of 1D Signals

In practice, only the real part $s(x)$ of the signal of the form $f(x)e^{jUx}$ is available. Under the consideration that $f(x)$ is smooth whose bandwidth is less than the modulation U, the complex signal $f(x)e^{jUx}$ can be obtained from the real part $s(x)$ through the use of the hilbert transform ($f(x)e^{jUx} = s(x) + j\hat{s}(x)$ where $\hat{s}(x)$ is the hilbert transform of $s(x)$). $f(x)e^{jUx}$ is called the analytic form of $s(x)$ and is to be used for analyzing the frequency contents of $s(x)$ by the modulated wavelet transform. Figure 1(a) shows a 1D test signal of 200 points composed of two emergent frequencies, $U=1$ in the first half and $U=2$ in the last half. The amplitude response is shown in Figure 1(b). By taking the modulated wavelet transform of its analytic form with several modulation frequencies ranging from 0.1 to π in two successive levels shown in Figures 1(c) and 1(d), respectively where the horizontal axis is the time axis, the vertical axis is the modulation frequency axis, the dark means small amplitude value and the bright means large amplitude value. It is found that, as one can expect, the amplitudes of the associated wavelet coefficients of the modulated wavelet transform reach to the minimum value while the modulation frequency equals to the emergent frequency of the signal. Figure 1(e) shows the estimate of the emergent frequency based on the proposed rule given by $\hat{U}(n) = \arg\left[\min_U \left\{\left|D_1(n)e^{j2U n}\right| + \left|D_2(n)e^{j2^2 U n}\right|\right\}\right]$ where $D_\ell(n)e^{j2^\ell Un}$ is the wavelet coefficient of the modulated wavelet

transform at resolution 2^{ℓ} modulated by U, and $\hat{U}$ is the estimate of the emergent frequency.

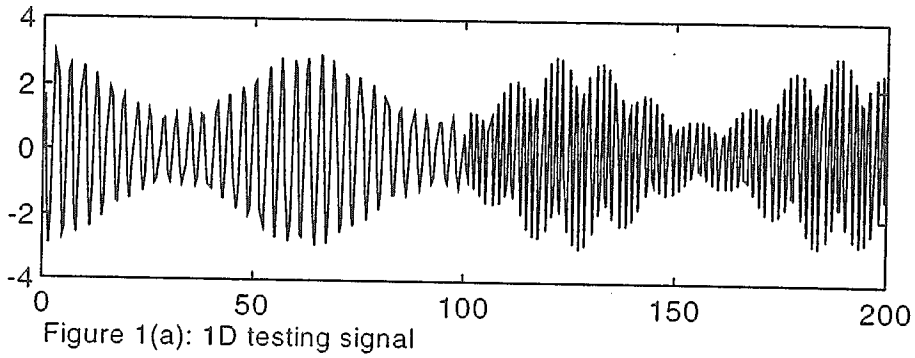

Figure 1(a): 1D testing signal

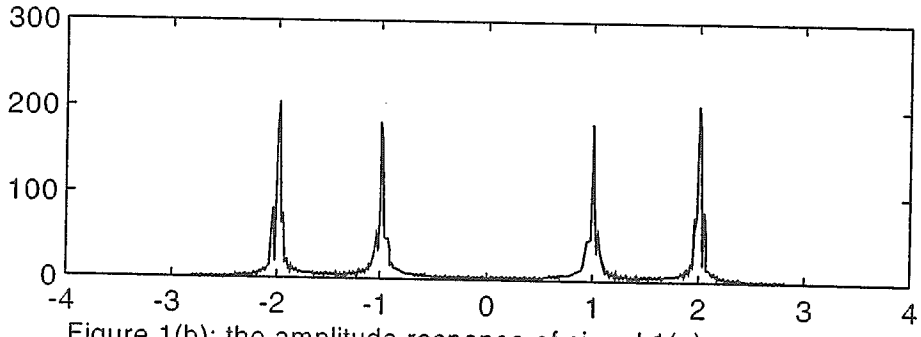

Figure 1(b): the amplitude response of signal 1(a)

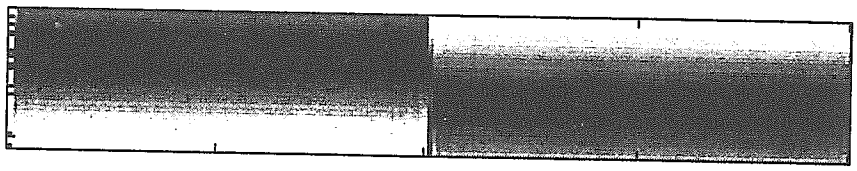

Figure 1(c): amplitude-frequency plane of the modulated wavelet transform of 1(a) in the first-level decomposition

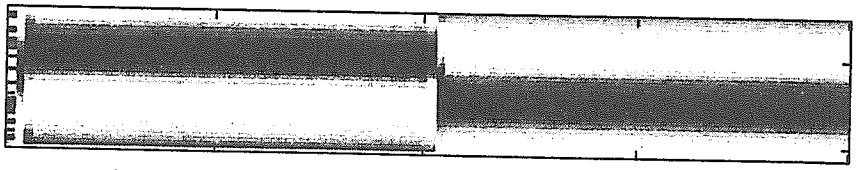

Figure 1(d): amplitude-frequency plane of the modulated wavelet transform of 1(a) in the second-level decomposition

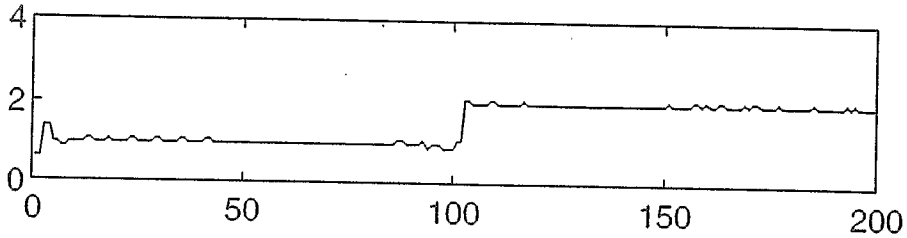

Figure 1(e): detection result of the emergent frequency of 1(a)

4.1 2D Modulated Wavelet Transform

The 2D wavelet transform obtained by the tensor product of two 1D wavelet transforms has one scaling function ($\phi(x,y)=\phi(x)\phi(y)$) and three wavelets ($\psi^1(x,y)=\phi(x)\psi(y)$, $\psi^2(x,y)=\psi(x)\ \phi(y)$ and $\psi^3(x,y)=\psi(x)\ \psi(y)$) [9]. For a 2D signal of the form $f(x,y)\ e^{j(U_x x+U_y y)}$, where $f(x,y)\in V_0$ is smooth and can be decomposed by

$$f(x,y)=\sum_{mn} S_J(m,n)\phi_{Jmn}(x,y)+\sum_{\ell=J}^{1}\sum_{k=1}^{3}\sum_{mn} D_\ell^k(m,n)\psi_{\ell mn}^k(x,y) \qquad (7)$$

where $S_\ell(m,n)$ and $D_\ell^k(m,n)$ are the scaling coefficients and wavelet coefficients of $f(x,y)$ at resolution 2^ℓ, respectively $\phi_{jmn}(x,y)=\phi_{jm}(x)\ \phi_{jn}(y)$, $\psi_{jmn}^k(x,y)=2^{-j}\psi^k(2^{-j}x-m,2^{-j}y-n)$; $k=1,2,3$ and J is the coarsest scale in decomposition. The 2D wavelet transform and the 2D inverse wavelet transform of $f(x,y)$ are given by

$$\begin{aligned} S_\ell(m,n) &= \sum_{p,q} S_{\ell-1}(p,q)h(2m-p)h(2n-q) \\ D_\ell^k(m,n) &= \sum_{p,q} S_{\ell-1}(p,q)g^k(2m-p,2n-q) \end{aligned} \qquad (8)$$

and

$$S_{\ell-1}(m,n) = \sum_{p,q} S_\ell(p,q)\tilde{h}(m-2p)\tilde{h}(n-2q)+\sum_{k=1}^{3}\sum_{p,q} D_\ell^k(p,q)\tilde{g}^k(m-2p,n-2q) \qquad (9)$$

, respectively where $g^1(m,n)=h(m)g(n)$, $g^2(m,n)=g(m)h(n)$, $g^3(m,n)=g(m)g(n)$, $S_\ell(m,n)=<f(x,y),\phi_{\ell mn}(x,y)>$, $D_\ell^k(m,n)=<f(x,y),\psi_{\ell mn}^k(x,y)>$, $\tilde{g}^k(m,n)=g^k(-m,-n)$ and $\tilde{h}(n)=h(-n)$; $k=1,2,3$. Based on equation (7), one can decompose such the 2D signal as follows,

$$\begin{aligned} f(x,y)e^{j(U_x x+U_y y)} = & \sum_{mn}(S_J(m,n)e^{j2^J(U_x m+U_y n)})\ \phi_{Jmn}(x,y)e^{j2^J U_x(2^{-J}x-m)}e^{j2^J U_y(2^{-J}y-n)}+ \\ & \sum_{\ell=J}^{1}\sum_{k=1}^{3}\sum_{mn}(D_\ell^k(m,n)e^{j2^\ell(U_x m+U_y n)})\ \psi_{\ell mn}^k(x,y)e^{j2^\ell U_x(2^{-\ell}x-m)}e^{j2^\ell U_y(2^{-\ell}y-n)} \end{aligned} \qquad (10)$$

which is called the 2D modulated wavelet decomposition by using the modulated scaling function $\phi_{\ell mn}(x,y)\ e^{j2^\ell U_x(2^{-\ell}x-m)}\ e^{j2^\ell U_y(2^{-\ell}y-n)}$ and the modulated wavelets $\psi_{\ell mn}^k(x,y)\ e^{j2^\ell U_x(2^{-\ell}x-m)}\ e^{j2^\ell U_y(2^{-\ell}y-n)}$; $k=1,2,3$, with the associated scaling coefficients $S_\ell(m,n)\ e^{j2^\ell(U_x m+U_y n)}$ and wavelet coefficients $D_\ell^k(m,n)\ e^{j2^\ell(U_x m+U_y n)}$ which represent the approximation information and detail information of $f(x,y)\ e^{j(U_x x+U_y y)}$ at resolution 2^ℓ, respectively. Based on equations (8) and (9), the 2D modulated wavelet transform and the 2D modulated inverse wavelet transform of $f(x,y)e^{j(U_x x+U_y y)}$ are given by

$$\begin{aligned} S_\ell(m,n)e^{j2^\ell(U_x m+U_y n)} &= \sum_{pq} S_{\ell-1}(p,q)e^{j2^{\ell-1}(U_x p+U_y q)}h(2m-p)\ e^{j2^{\ell-1}U_x(2m-p)}h(2n-q)e^{j2^{\ell-1}U_y(2n-q)} \\ D_\ell^k(m,n)e^{j2^\ell(U_x m+U_y n)} &= \sum_{pq} S_{\ell-1}(p,q)e^{j2^{\ell-1}(U_x p+U_y q)}\ g^k(2m-p,2n-q)e^{j2^{\ell-1}U_x(2m-p)}e^{j2^{\ell-1}U_y(2n-q)} \end{aligned} \qquad (11) \text{ and}$$

$$\begin{aligned} S_{\ell-1}(m,n)e^{j2^{\ell-1}(U_x m+U_y n)} = & \sum_{pq} S_\ell(p,q)e^{j2^\ell(U_x p+U_y q)}\tilde{h}(m-2p)\ e^{j2^{\ell-1}U_x(m-2p)}\tilde{h}(n-2q)e^{j2^{\ell-1}U_y(n-2q)}+ \\ & \sum_{k=1}^{3}\sum_{pq} D_\ell^k(p,q)e^{j2^\ell(U_x p+U_y q)}\tilde{g}(m-2p,n-2q)\ e^{j2^{\ell-1}U_x(m-2p)}e^{j2^{\ell-1}U_y(n-2q)} \end{aligned} \qquad (12), \text{ respectively.}$$

4.2 Experimental Results in Texture Segmentation

The original textured image data are taken as the scaling coefficients $S_0(m,n)$ for the standard wavelet transform and taken as the scaling coefficients $S_0(m,n)e^{j(U_k m+V_k n)}$ for the modulated wavelet transform with the modulation frequency (U_k,V_k), both coefficients are at the finest resolution 2^0. Daubechies scaling function D8 and the corresponding $h-$ and $g-$ filters are used. The absolute values of the wavelet coefficients associated with the standard wavelet transform and those associated with the modulated wavelet transform are used as features by K-means clustering algorithm, in an unsupervised mode, to segment textured images. Figure 2(a) shows an image composed of four textures in different orientations (0^o, 90^o, 45^o and -45^o). The segmentation result (Figure 2(b)) based on the standard wavelet transform shows that the textures of 45^o and -45^o orientations can not be discriminated. The orientation characteristics of textures can be taken into account by including the wavelet coefficients associated with the modulated wavelet transform with the modulation frequency ($\pi/2, -\pi/2$). The improvement in segmenting such type

of textured images is shown in Figure 2(c), and the boundary between segmented regions with small errors of from 1 to 3 pixels is shown in Figure 2(d). Figure 3(a) is another test image consisting of five different textures. Figure 3(b) is the segmentation result based only on the standard wavelet transform resulting in two textures are unable to be segmented. By including the orientation selectivity provided by the modulated wavelet transform with the modulation frequency $(\pi/2, -\pi/2)$, the segmentation is improved (Figure 3(c)) and the boundaries among the segmented regions is shown in Figure 3(d). The last experiment is performed on a cloud image shown in Figure 4(a) which is a part of a remotely sensed image of clouds over North Sea. The spread of the cold air appears on the left and the cloud streets of a cyclone on the right. Segmentation is done by clustering the amplitudes of the wavelet coefficients of the standard wavelet transform and those of the modulated wavelet transform with the modulation frequency $(\pi/2, -\pi/2)$ in two-level decomposition. The segmentation result is shown in Figure 4(b) and the texture border of the cold air area is quite well localized as shown in Figure 4(c).

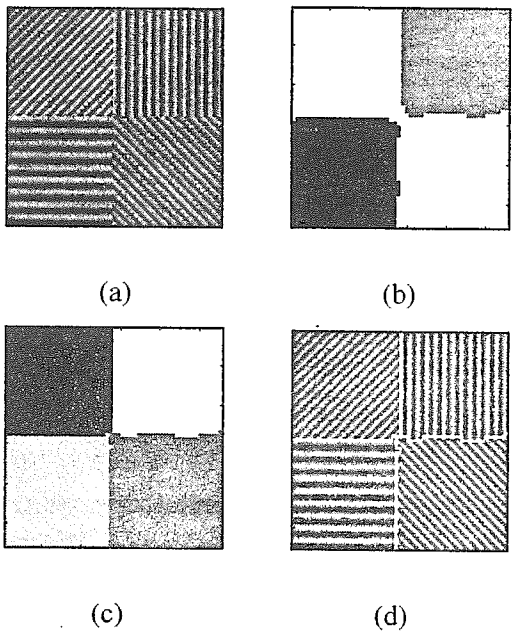

(a) (b)

(c) (d)

Figure 2: test image (a); the segmentation result by using the standard wavelet transform (b); the segmentation result by including the modulated wavelet transform (c); boundary of the segmented regions in figure (c) (d).

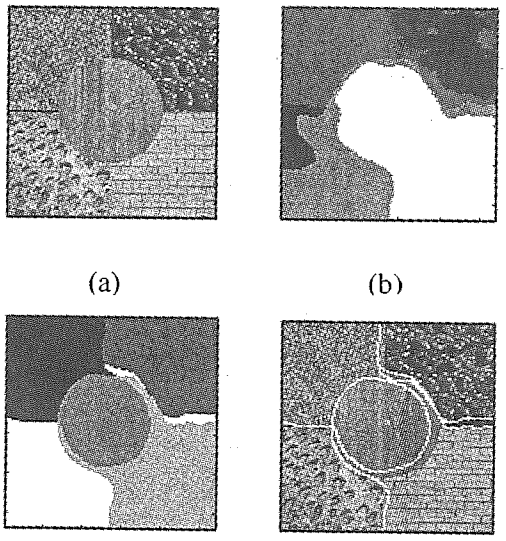

(a) (b)

(c) (d)

Figure 3: test image (a); the segmentation result by using the standard wavelet transform (b); the segmentation result by including the modulated wavelet transform (c); boundary of the segmented regions in figure (c) (d).

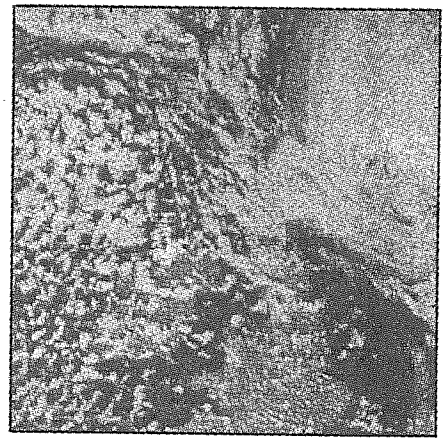

(a)

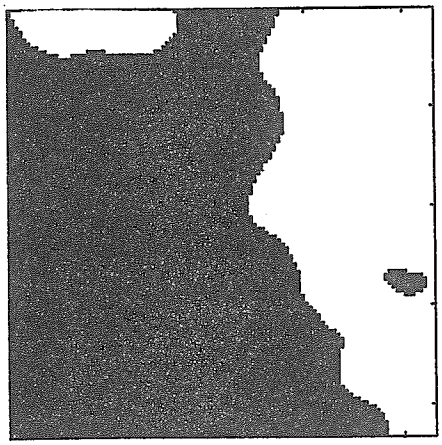

(b)

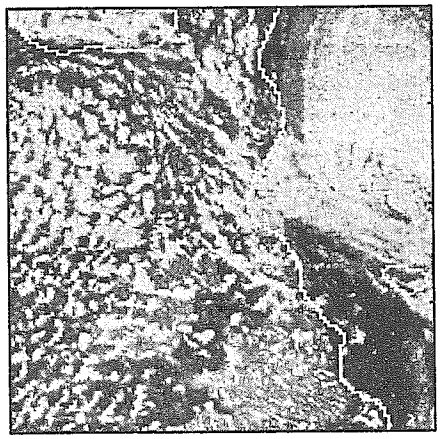

(c)

Figure 4: the cloud image (a); the segmentation result by including the modulated wavelet transform (b); boundary of the segmented regions in figure (b) (c).

5. Conclusions

Signals which are globally nonstationary but locally coherent in terms of the frequency characteristics can be modeled by modulating a smooth function with a slow-varying modulation frequency. The modulated wavelet transform for such signals provides a time-frequency-like analysis. The textured images modeled by modulating a smooth function, representing the slow-varying illumination, with a significant modulation frequency determined by the surface characteristics of textures are considered. It is shown that the segmentation of textures is improved by including the orientation selectivity through use of the modulated wavelet transform.

References

[1] A. C. Bovik, M. Clark and W. S. Geisler, "Multichannel Texture Analysis Using Localized Spatial Filters," IEEE Trans. on PAMI, vol. 12, no. 1, pp. 55-73, 1990.

[2] Dennis Dunn and William E. Higgins, "Optimal Gabor Filters for Texture Segmentation," IEEE Trans. on Image Processing, vol. 4, no. 7, pp. 947-964, 1995.

[3] A. Teuner, et al., "Unsupervised Texture Segmentation of Images Using Tuned Matched Gabor Filters," IEEE Trans. on Image Processing, vol. 4, no. 6, pp. 863-870, 1995.

[4] Michael Unser and Murray Eden, "Multiresolution Feature Extraction and Selection for Texture Segmentation," IEEE Trans. on PAMI, vol. 11, no. 7, pp. 717-728, 1989.

[5] Charles Bouman and Bede Liu, "Multiple Resolution Segmentation of Textured Images," IEEE Trans. on PAMI, vol. 13, no. 2, pp. 99-113.

[6] S. Krishnamachari and R. Chellappa, "Multiresolution Gauss Markov Random Field Models for Texture Segmentation," IEEE Trans. on I P, vol. 6, no. 2, pp. 251-267, 1997.

[7] B. S. Manjunath and R. Chellappa, "Unsupervised Texture Segmentation Using Markov Random Fields," IEEE Trans. on PAMI, vol. 13, pp. 478-482, 1991.

[8] C. S. Won and H. Derin, "Unsupervised Segmentation of Noisy and Textured Images Using Markov Random Fields," CVGIP, vol. 54, no. 4, pp. 308-328, 1992.

[9] S. Mallat, "A Theory for Multiresolution Signal Decomposition: The Wavelet Representation," IEEE Trans. on PAMI, vol. 11, no. 7, pp. 674-693, 1989.

[10] G. Strang, "Wavelets and Dilation Equations: A Brief Introduction," SIAM Review, vol. 31, no. 4, pp. 614-627. 1989.

[11] I. Daubechies, "Orthonormal Bases of Compactly Supported Wavelets," Comm. in Pure Appl. Math. vol. 41, pp. 909-996, 1988.

[12] T. Chang and C. C. J. Kuo, "A Wavelet Transform Approach to Texture Analysis," Proc. IEEE ICASSP, San Francisco, CA., pp. 661-664, 1992.

[13] A. Laine and J. Fan, "Texture Classification by Wavelet Packet Signatures," TR-92-023, Center for Computer Vision and Visualization, University of Florida, June, 1992.

[14] His-Chin Hsin and Ching-Chung Li, "An Experiment on Texture Segmentation using Modulated Wavelets," IEEE Inter. Conf. on SMC, vol. 4, pp. 529-534, France, 1993.